

# Nonlinear lossy light bullets in self-focusing media with nonlinear absorption

Miguel A. Porras

*Grupo de Sistemas Complejos, ETSIME, Universidad Politécnica de Madrid, Ríos Rosas 21, 28003 Madrid, Spain*

We review the properties of nonlinear, multidimensional localized waves whose stationary propagation is sustained by a dynamic equilibrium between self-focusing and nonlinear losses. Their finite-energy versions preserve light bullet behavior well-beyond the characteristic diffraction or dispersion distances, and rebuild after obstacles. There exists a preferential lossy light bullet with maximum intensity and losses, defined solely by the optical properties of the medium, which is the most stable, non-conical localized wave supported by a medium with self-focusing nonlinearity and nonlinear losses. This preferential lossy light bullet acts as an attractor during self-focusing of Gaussian-like wave packets when collapse is halted by nonlinear absorption, which can explain relevant properties of the observed light filament dynamics in media with anomalous dispersion.

## I. INTRODUCTION

In this article we review the properties of the so-called nonlinear lossy light bullets (LLBs). They constitute a family of localized and non-diffractive light wave packets in homogeneous, isotropic, nonlinear media that results from a dynamic balance between energy dissipation and self-focusing [1, 2]. Their properties differ substantially from those of other, well-known families of non-diffractive, nonlinear light bullets, as solitary, conical and dissipative bullets. LLBs are substantially nonlinear and multidimensional waves (2D and 3D), and feature a rather complex spatiotemporal structure. They survive to nonlinear absorption and rebuild after obstacles, but these properties do not result from a peculiar geometry, as in conical light bullets [3–8], or on a balancing gain, as in dissipative light bullets [9–11]. The stationary propagation of LLBs against nonlinear losses is a result of the refilling effect of self-focusing. Self-focusing establishes an energy flux from an energy reservoir in the light bullet periphery towards the nonlinearly absorbed central core of the bullet. Further, nonlinear losses make the propagation of these LLBs more robust against perturbations. In each nonlinear medium, there exists a LLB with maximum intensity and maximum losses, defined by the optical properties of the medium solely, that exhibits maximum stability properties, and that act as an attractor of the self-focusing dynamics with nonlinear losses. The existence of this attractor can explain many facts of the self-focusing, collapse and filamentation dynamics when collapse is arrested by nonlinear losses [12–14].

Along this paper, these properties and their relevance in experiments are reviewed. In Sections II and III we introduce LLBs as localized and stationary solutions of the two or three dimensional nonlinear Schrödinger equation with self-focusing nonlinearity and nonlinear losses, and describe their rather complex structure, formed by a narrow peak, surrounded by a dissipative shell and an energy reservoir. In the LLB with maximum intensity and maximum losses supported by the medium, the dissipative shell extends infinitely far from the bullet center. The propagation properties of the physically realizable, finite-energy versions of LLBs are studied in Section IV,

where it is seen that truncated LLBs can propagate as light bullets for hundreds of diffraction lengths. Section V describes the self-reconstruction property of LLBs after obstacles. Special attention is paid to the difficult question of the stability of LLBs. In Section VIA we show that the LLB of maximum intensity and losses tends to be spontaneously formed in the collapse of standard wave packets with finite energy arrested by nonlinear losses [1, 15]. The dynamics towards the formation, and relaxation from this LLB attractor is seen to reproduce many features of the filamentation dynamics of monochromatic light (in the two-dimensional case), and of the filamentation dynamics of ultrashort pulses in media with anomalous dispersion (in the three-dimensional case), as the filament intensity, the particularly long segments and revivals in the form of short bursts. The stability properties of LLBs are studied in Section VIB by means of a linearized instability analysis. As expected from its attractive property, the LLB of maximum intensity and losses turns out to be the most stable among all LLBs.

## II. LOSSY LIGHT BULLETS IN SELF-FOCUSING MEDIA WITH NONLINEAR LOSSES

We consider wave packets  $E = A \exp(-i\omega_0 t + ik_0 z)$  oscillating a certain optical carrier frequency  $\omega_0$  and of propagation constant  $k_0$ , that self-focus symmetrically in all available dimensions. In two dimensions, this represents a monochromatic light beam  $A(r, z)$  that depends only on the radial coordinate  $r = (x^2 + y^2)^{1/2}$  in the transversal plane. In three-dimensions, self-focusing is symmetric in a medium with anomalous dispersion [ $k_0'' < 0$ ] if the envelope  $A(r, z)$  depends only on the spatiotemporal radial coordinate  $r = (x^2 + y^2 + t'^2/k_0|k_0''|)^{1/2}$ , where  $t' = t - k_0' z$  is the local time and  $k_0^{(n)}$  is the  $n$ th-derivative of the propagation constant  $k(\omega)$  at  $\omega_0$ . Two-dimensional symmetrical self-focusing in a planar wave can be considered as well if  $r = (x^2 + t'^2/k_0|k_0''|)^{1/2}$ . In all these cases, the simplest model of self-focusing is the

nonlinear Schrödinger equation (NLSE)

$$\partial_z A = \frac{i}{2k_0} \Delta_r A + \frac{ik_0 n_2}{n_0} |A|^2 A - \frac{\beta^{(M)}}{2} |A|^{2M-2} A, \quad (1)$$

where  $\Delta_r = \partial_r^2 + [(D-1)/r]\partial_r$ , with  $D = 2$  or  $D = 3$ , and  $n_0$  is the refractive index at  $\omega_0$ . A pure Kerr nonlinearity with nonlinear refractive index  $n_2 > 0$  is considered for simplicity, but other more complex self-focusing nonlinearities can be considered as well. The term with  $\beta^{(M)} > 0$  accounts for nonlinear losses (NLLs) due to  $M$ -photon absorption.

The NLSE (1) supports localized and stationary solutions of the form  $A = a(r) \exp[i\varphi(r) + i\delta z]$ , where  $a$  and  $\varphi$  are real functions, with  $\delta > 0$  in completely transparent media (solitons), and with  $\delta < 0$  also in media with NLLs (linear or nonlinear conical waves) [3, 7, 8, 16]. Between these two families, Eq. (1) supports also localized and stationary solutions without any axial wave vector shift ( $\delta = 0$ ) in nonlinear media with NLLs, that have been named lossy light bullets [1, 2], and that present substantially different characteristics from solitary or conical bullets. From Eq. (1), these LLBs must satisfy

$$a'' + \frac{D-1}{r} a' - \varphi'^2 a + \frac{2k_0^2 n_2}{n_0} a^3 = 0, \quad (2)$$

$$\beta^{(M)} \int_0^r dr \pi (2r)^{D-1} a^{2M} = -\frac{\pi (2r)^{D-1}}{k_0} \varphi' a^2 \quad (3)$$

where prime signs stand for  $d/dr$ , with boundary conditions with  $a(0) = \sqrt{I_0}$ ,  $a'(0) = 0$ ,  $\varphi'(0) = 0$ , and with the additional localization condition  $a \rightarrow 0$  for  $r \rightarrow \infty$ . These solutions are numerically to exist in two and three dimensions for all peak intensity  $I_0$  up to the maximum value

$$I_{0,\max} = \left[ \frac{4\gamma_{\max} k_0 n_2}{n_0 \beta^{(M)}} \right]^{\frac{1}{M-2}}, \quad (4)$$

where  $\gamma_{\max}$  is a dimensionless parameter of the order of unity that depends slightly on  $M$  and number of dimensions  $D$ . Contrary to solitons, there no exist solutions to Eqs. (2) and (3) satisfying the localization condition in the case of only one dimension.

Radial profiles for  $D = 2$  and  $M = 6$  with different values of  $I_0$  between the limits  $I_0 \rightarrow 0$  of negligible losses (lower dashed curve) and  $I = I_{0,\max}$  (upper dashed curve) are shown in Figs. 1(a) and (b). Qualitatively similar profiles are found for different values of  $M$  and for  $D = 3$ . LLBs are weakly localized so that they carry infinite power (in two dimensions) or energy (in three dimensions). Equation (3), written as  $N(r) = -F(r)$  for short, establishes that the nonlinearly absorbed power (energy)  $N(r)$  per unit propagation length in any circle (sphere) of radius  $r$  must be refueled by identical inward radial power (energy) flux  $-F(r)$  per unit length across the circumference of the circle (surface of the sphere) for stationarity to be possible. This mechanism of stationarity with NLLs was first described for conical

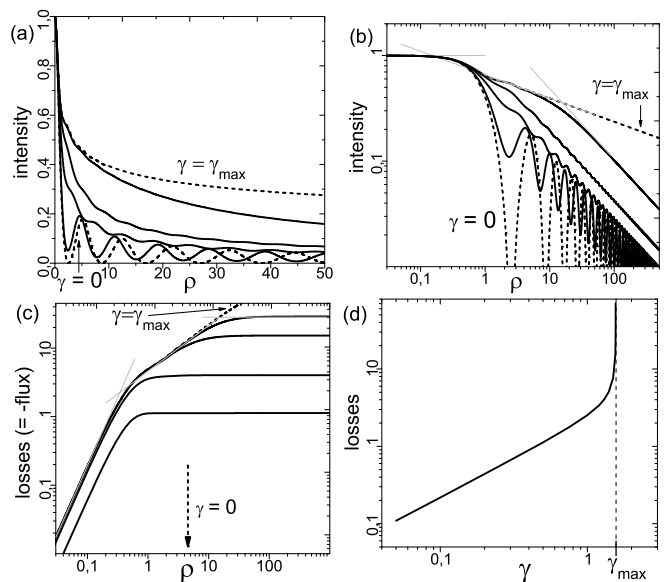


FIG. 1. (a) normalized intensity, (b) normalized intensity in double logarithmic scale, and (c) normalized NLLs (or normalized inward power flux) radial profiles of LLBs with  $M = 6$  and  $D = 2$ . The dashed curves correspond to the limiting cases of negligible and infinite losses. They are obtained by solving (2) and (3) in the dimensionless form  $\tilde{a}'' + (D-1)\tilde{a}'/\rho - \varphi'^2 \tilde{a} + 2\tilde{a}^3 = 0$ , and  $-\pi(2\rho)^{D-1}\varphi' \tilde{a}^2 = 4\gamma \int_0^\rho d\rho \pi (2\rho)^{D-1} \tilde{a}^{2M}$  (normalized inward flux = normalized losses), where  $\tilde{a} = a/\sqrt{I_0}$ ,  $\rho = \sqrt{k_0^2 n_2 I_0/n_0} r$  is the normalized radial coordinate, and with different values of  $\gamma = n_0 \beta^{(M)} I_0^{M-2}/4k_0 n_2 = 0.5, 1.3, 1.5, 1.558$  between the limits  $\gamma = 0$  and  $\gamma = \gamma_{\max} = 1.5594$  for  $M = 6$  and  $D = 2$ . (d) Normalized total NLLs, or normalized total inward flux, per unit propagation length as a function of  $\gamma$  (or peak intensity) up to the limiting value  $\gamma_{\max}$  (or  $I_{0,\max}$ ) of existence of LLBs.

bullets ( $\delta < 0$ ) [7, 8], but the existence of the LLBs evidences that it can also work without an inward conical flux. The loss profiles  $N(r)$  of the LLBs of Fig. 1(a) are represented in Fig. 1(c). LLBs loss a finite fraction  $N_T = N(r \rightarrow \infty)$  of their infinite power (energy) per unit propagation length, at the same time that a power (energy) flux  $-F_T = N_T$  comes from large radial distances towards the center to compensate these losses. The value  $-F_T = N_T$  is indicated as a horizontal gray straight line in Fig. 1(c), and their values are represented in Fig. 1(d) for the different values of the peak intensity  $I_0$ . Only in the limit  $I_0 = I_{0,\max}$ , the localization of the lossy light bullet is so weak that both the power and the NLLs per unit propagation are infinite.

### III. THE STRUCTURED PROFILE OF LOSSY LIGHT BULLETS AND THEIR ENERGY RESERVOIR

While in conical light bullets stationarity with NLLs is due to an overweight of the linear conical part push-

ing energy inward with respect to the conical part pushing outward, in LLBs these contributions to the energy flux are not separable because of the nonlinear origin of the energy flux. The dynamic balance of NLLs and self-focusing requires the structured radial profiles revealed in the double logarithmic plots of Figs. 1 (b) and (c), where three sequential scaling power-laws ( $\propto r^{-\sigma}$ ) with different scaling powers  $\sigma$  can be appreciated in each profile (gray straight lines).

First, while the intensity  $a^2(r)$  remains of the order of  $I_0$  in the vicinity of  $r = 0$  [horizontal straight line in Fig. 1(b)], Eq. (3) yields  $-F(r) = N(r) \simeq (2^{D-1}\pi r^D/D)\beta^{(K)}I_0^{(K)}$  [steepest straight line in (c)], and this flux requires wave fronts  $\varphi(r) \simeq \varphi(0) - k_0\beta^{(K)}I_0^{K-1}r^2/2D = \text{const.}$ , i.e., spherical wave fronts with the same curvature  $1/R = \beta^{(K)}I_0^{K-1}/D$  at any propagation distance. About  $r = 0$ , Eq. (2) reduces asymptotically to  $a'' + (D-1)a'/r + (2k_0^2n_2/n_0)a^3 \simeq 0$ . The shape of the central peak is then substantially independent of the dissipative properties of the medium, and its width,  $\Delta r \simeq [\ln(2)n_0D/2k_0^2n_2I_0]^{1/2}$  (HWHM), is approximately equal to the width of the ground solitons in two (Townes beam) and in three dimensions with the same peak intensity  $I_0$  in transparent media. The central peak of the LLB thus resembles a propagating soliton, but it is actually being continuously absorbed and replenished due to the flux created by its converging wave fronts.

Second, replenishment of the whole central peak requires a larger flux coming from around [Figs. 1(b) and (c), intermediate straight lines]. If we write the power law of the shell around the central peak as  $a \simeq br^{-\sigma}$ , where  $b$  is a constant, Eq. (3) yields  $-F(r) = N(r) \simeq cr^{D-2M\sigma}$ , where  $c = \beta^{(M)}\pi 2^{D-1}b^{2M}/(D-2M\sigma)$ . This requires converging (but non-spherical) wave fronts with  $\varphi'(r) \simeq -dr^{1-2(M-1)\sigma}$ , where  $d = k_0\beta^{(M)}b^{2M-2}/(D-2M\sigma)$ . From Eq. (2), the relation  $-d^2r^{2-4\sigma(M-1)} + (2k_0^2n_2b^2/n_0)r^{-2\sigma} \simeq 0$  is found as the condition for the strength of self-focusing to be consistent with these wave fronts. Equating the exponents and the constants of the two terms, one readily obtains

$$\sigma_S = \frac{1}{2M-3}, \quad b_S = \left[ \sqrt{\frac{2n_2}{n_0}} \frac{(D-2M\sigma)}{\beta^{(M)}} \right]^{\frac{1}{2M-3}}, \quad (5)$$

for the power-law  $a \simeq b_S r^{-\sigma_S}$  of the amplitude in the shell surrounding the peak [intermediate straight line in Figs. 1(b)]. This shell is wider, and the losses higher, as the peak intensity  $I_0$  approaches  $I_{0,\text{max}}$ , becoming infinitely wide and high for the lossy light bullet with  $I_0 = I_{0,\text{max}}$  [dashed lines in Figs. 1(b) and (c)].

Except for the lossy light bullet with  $I_0 = I_{0,\text{max}}$ , the outer part of the lossy light bullet is characterized by the absence of absorption, since the inward flux reaches a constant value  $-F_T = N_T$  that compensates the total NLLs  $N_T$ . Proceeding as above but replacing  $N(r)$  with  $N_T$  at large  $r$ , one finds  $\varphi'(r) \simeq -dr^{2\sigma-D+1}$ , where  $d = k_0N_T/2^{D-1}\pi b^2$ , for the converging wave fronts, and the

balance relation  $-d^2r^{4\sigma-2D+2} + (2k_0^2n_2b^2/n_0)r^{-2\sigma} \simeq 0$  for the self-focusing state with these wave fronts. From this relation we find

$$\sigma_a = \frac{D-1}{3}, \quad b_a = \left( \frac{N_T^2 n_0}{2^{2D-1}\pi^2 n_2} \right)^{1/6}, \quad (6)$$

for the asymptotic power-law  $a \simeq b_a r^{-\sigma_a}$  at large  $r$  [steepest straight line in Fig. 1(b)]. LLBs are then nonlinear waves also asymptotically. Self-focusing is continuously pushing the power (energy) contained in this huge, widespread, and non-absorbed reservoir to replenish the total lost power (energy) in the center.

In the context of the cubic-quintic Ginzburg-Landau equation, dissipative solitons with permanently converging wave fronts have also been described in the two-dimensional case [9–11]. However, these dissipative solitons carry finite power, and their stationarity is based on a balance between the losses and gain that take place in different parts of their radial profiles.

The radial oscillations accompanying the asymptotic decay of LLBs [Figs. 1(a) and (b)] have also little to do with the linear oscillations of conical bullets. An asymptotic analysis similar to that described above shows that both the amplitude and frequency of the nonlinear oscillations are proportional to the field amplitude  $b_a r^{-\sigma_a}$ . The amplitude and frequency of the oscillations follow then the same scaling power law with power  $(D-1)/3$ , in contrast with the amplitude decay with power  $(D-1)/2$  and the constant frequency of the oscillations of conical light bullets. More precisely, at each radius  $r$ , the local radial frequency  $K = (k_x^2 + k_y^2)^{1/2}$ , or spatiotemporal radial frequency  $K = [k_x^2 + k_y^2 + k_0|k_0''|(\omega - \omega_0)^2]^{1/2}$  of the oscillations about  $b_a r^{-\sigma_a}$  are given by

$$K(r) \simeq k_0 \sqrt{\frac{12n_2}{n_0}} b_a r^{-\sigma_a}. \quad (7)$$

LLBs contain then a continuous of frequencies in its spectrum, with decreasing frequencies distributed along the radial profile at increasingly larger distances from the bullet center.

### A. The most lossy light bullet in a nonlinear dissipative medium

Oscillations cease in the limit of peak intensity  $I_0$  equal to  $I_{0,\text{max}}$ . As we will see in Sec. VIA, this limiting bullet with infinite power and infinite losses is, despite its ideal nature, of particular relevance in the self-focusing of real (finite-energy) wave packets in media with NLLs. Its peak intensity, given by Eq. (4), depends only on the number of dimensions and the optical properties of the medium at the carrier wave length. The lossy shell extends up to infinite radial distances, and therefore its asymptotic decay follows the power law specified by Eq. (5), which depends only on the number of dimensions and the optical properties of the medium.

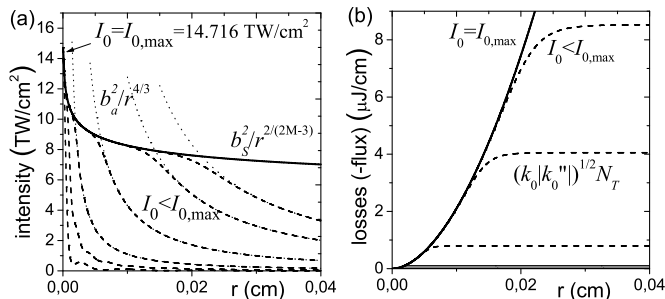


FIG. 2. Solid thick curves: (a) Intensity and (b) nonlinear loss profiles  $(k_0|k_0''|)^{1/2}N(r)$  [equal to the inward energy flux profile  $-(k_0|k_0''|)^{1/2}F(r)$ ] of the most lossy three-dimensional light bullet, whose intensity is  $I_0 = I_{0,\max} = 14.716$  TW/cm<sup>2</sup> [Eq. (4) with  $\gamma_{\max} = 3.15294$  for  $D = 3$  and  $M = 10$ ] in fused silica at 1550 nm carrier wave length ( $k_0 = 5.854 \times 10^4$  cm<sup>-1</sup>,  $k_0'' = -279.4$  cm<sup>-1</sup>fs<sup>2</sup>,  $n_2 = 2.2 \times 10^{-16}$  cm<sup>2</sup>/W,  $\beta^{(M)} = 5.11 \times 10^{-116}$  cm<sup>17</sup>/W<sup>9</sup>, and  $M = 10$ ). Dashed thick curves: Intensity and nonlinear loss profiles of LLBs with slightly lower peak intensities  $I_0$ , for comparison.

For reference in Section VIA, the solid curves in Figs. 2(a) and (b) represent the radial profiles of intensity and NLLs (-flux) of the most lossy, three-dimensional light bullet in fused silica at 1550 nm carrier wavelength ( $M = 10$ ). The intensity asymptotic decay  $b_S^2/r^{2/(2M-3)} = b_S^2/r^{2/17}$  is much slower than the intensity asymptotic decays  $b_a^2/r^{2(D-1)/3} = b_a^2/r^{4/3}$  (dotted curves) of the LLBs of lower intensity, shown in Fig. 2(a) as dashed curves.

#### IV. PROPAGATION PROPERTIES OF PHYSICALLY REALIZABLE LOSSY LIGHT BULLETS

Since LLBs carry infinite energy, only approximate versions with finite energy can be formed in practice. As seen in Sec. VI, LLBs with  $I_0$  close to  $I_{0,\max}$  are spontaneously formed, but only up to a maximum radial distance  $r_t$ , from the finite-energy of collapsing Gaussian-like wave packets in media with NLLs.

The propagation properties of these truncated LLBs can be understood from the structure described above. For example, Fig. 3(a) shows the spectrum of radial frequencies of two-dimensional LLBs truncated at different radii  $r_t$ . Truncation removes the frequencies  $K < K(r_t)$  distributed at  $r > r_t$ , as in a low-pass filter. This causes the frequencies  $K \simeq K(r_t)$  distributed about the truncation radius  $r_t$  to dominate, since they fill the largest area or volume. The spectrum then resembles the annular spectrum of a conical wave with a main cone angle  $K(r_t)/k_0$  determined by the truncation radius. This may be the reason why LLBs with finite radius can easily be interpreted as (linear or nonlinear) Bessel beams in self-focusing experiments [17]. The frequency spectrum

of truncated LLBs differ from those of truncated conical bullets in that higher frequencies,  $K > K(r_t)$ , placed at  $r < r_t$  have more weight than in conical waves. Indeed, a truncated lossy light bullet behaves very much as a continuous of conical light bullets with cone angles equal or larger than  $K(r_t)/k_0$ , as seen below.

Despite the central peak of the lossy light bullet is continuously being absorbed, it can propagate without significant change for hundred times the diffraction length  $k_0(\Delta r)^2/2$  associated to its width (in the radially symmetric two-dimensional case), or hundred times the dispersion length, equal to the diffraction length, associated to its duration (in the spatiotemporal radially symmetric three-dimensional case). The distance of light bullet behavior  $L$  is determined by the distance at which the energy reservoir of the truncated lossy light bullet is consumed. For example, taking the truncated LLBs with the spectra of Fig. 3(a) as initial conditions, the evolution of the peak intensity along  $z$  according to the NLSE (1) is plotted in Fig. 3(b), where the normalized axial coordinate in Fig. 3(b) is such that the diffraction length associated to the width of the central peak is unity.

To estimate the distance  $L$  we consider the truncated lossy light bullet as a superposition of conical waves with cone angles  $\theta \simeq K(r)/k_0 \geq K(r_t)/k_0$ . Thus, the power coming from a position  $r < r_t$  in the initial condition reaches the center of the bullet, refilling it, at the diffraction-free distance  $r/\theta = k_0 r/K(r)$  [3], or from Eq. (7), at  $k_0 r^{(D+2)/3}/\sqrt{12}b_a$ . In particular, the power coming from the bullet border  $r_t$  reaches the center at the longest distance

$$L = \frac{k_0}{\sqrt{12}b_a} r_t^{\frac{D+2}{3}}, \quad (8)$$

which estimates the distance at which the power reservoir is completely consumed, and therefore the central peak initiates to decay. As seen in Fig. 3(b), Eq. (8) gives indeed the distance at which the peak intensity initiates to disappear. Unlike conical waves, the light bullet distance  $L$  grows faster than linearly with truncation radius, and depends also on the parameter  $b_a$  related to the total NLLs  $N_T$  per unit propagation length of the specific LLB.

#### V. SELF-RECONSTRUCTION PROPERTY

As conical bullets [4], LLBs have the property of rebuilding after being partially blocked. The dashed curve in Fig. 4(a) represents a two-dimensional lossy LLB with a hole of radius  $r_t$  comparable to that of the central peak, and the solid curve the propagated field from the NLSE (1) at a distance where the central peak is reconstructed. The self-reconstruction distance can be estimated following a similar reasoning as above. The peak initiates to rebuild when the power surrounding the hole begins to reach the center. For the different cone angles  $K(r)/k_0$

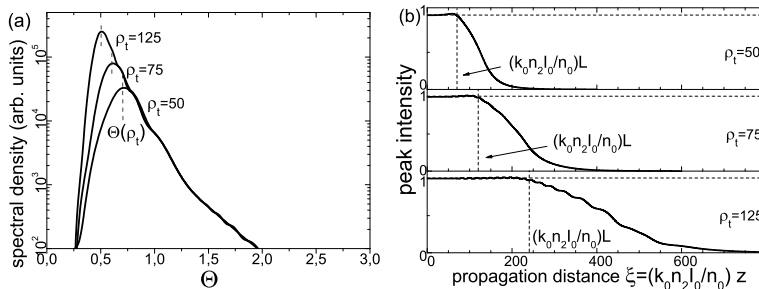


FIG. 3. (a) Radial spectral intensity of two-dimensional LLBs  $\tilde{a} \exp(i\varphi)$  with  $D = 2$ ,  $M = 6$  and  $\gamma = 1.3$ , truncated at different radii  $\rho_t$ . The truncation function is the super-Gaussian function  $\exp(-\rho^4/\rho_t^4)$ . The maxima are located at the local frequency  $K(\rho_t)$  at the truncation radius  $\rho_t$  (vertical segments) as given by Eq. 7. The normalized radial frequency in the graphic is  $\Theta = K/\sqrt{k_0^2 n_2 I_0 / n_0}$ . (b) Axial evolution of the peak intensity for the truncated LLBs in (a). It has been obtained by solving the NLSE (1) in the dimensionless form  $\partial_\xi \tilde{A} = (i/2)\Delta_\rho \tilde{A} + i|\tilde{A}|^2 \tilde{A} - 2\gamma|\tilde{A}|^{2M-2} \tilde{A}$  taking truncated LLBs  $\tilde{A}(\rho, 0) = \tilde{a} \exp(i\varphi) \exp(-\rho^4/\rho_t^4)$  as initial conditions. The normalized amplitude  $\tilde{a}$ , phase  $\varphi$ , radius  $\rho$ , and  $\gamma$  are defined in Fig. 1. The normalized axial coordinate is  $\xi = (k_0 n_2 I_0 / n_0) z$ . The dashed vertical segments indicate the light bullet propagation distances  $L$  for each truncation  $\rho_t$  predicted by Eq. (8).

at different radii  $r \geq r_t$ , the shortest axial distance of arrival of power corresponds to  $r_t$ , and is then given again by Eq. (8), with  $r_t$  standing now for the radius of the hole. For several two-dimensional LLBs with different peak intensities  $I_0$  and blocked up to a given radius  $r_t$ , Fig. 4(b) evidences that the peak intensity rises from zero up to the corresponding unblocked values  $I_0$  at a distance that is well approached by Eq. (8). Being equal the hole radii, different values of  $L$  are due only to different values of  $b_a$ , i.e., the different total NLLs  $N_T$  of the input LLBs. Of course, these numerical simulations have been performed in a grid of finite radius, and therefore the self-reconstruction property holds for LLBs with finite power.

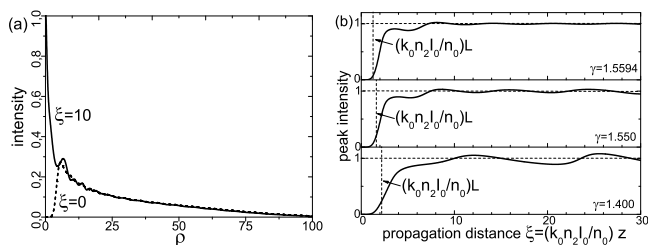


FIG. 4. (a) LLB  $\tilde{a} \exp(i\varphi)$  with  $D = 2$ ,  $M = 6$  and  $\gamma = 1.5$  (dashed curve) blocked up to  $\rho_t = 4$  with block function  $1 - \exp(-\rho^4/\rho_t^4)$ , and its propagated field (solid curve). (b) Change of the peak intensity with propagation distance for the LLBs with  $D = 2$ ,  $M = 6$  and  $\gamma = 1.5594, 1.55, 1.4$ , all blocked up to the same radius  $\rho_t = 4$ . Normalized field, propagation equation, coordinates and parameters are as in Figs. (1) and (3). The dashed vertical lines indicate the estimate of self-reconstruction distances  $L$  given by Eq. (8).

## VI. STABILITY PROPERTIES

Since LLBs are nonlinear waves, they can suffer from stabilities when they are perturbed, e. g., by truncation at  $r > r_t$  or by obscuration at  $r < r_t$ , as in the preceding sections. In fact, rebuilding of the central peak is seen in Fig. 4(b) to be accompanied by nonlinear oscillations, but these oscillations disappear as the intensity  $I_0$  of the rebuilding lossy light bullet approaches  $I_{0,\max}$ . Also, the truncated LLBs of Fig. 3(b) develop nonlinear oscillations, but again their growth rate is smaller as  $I_0$  approaches the limit  $I_{0,\max}$ . In this section we show that NLLs confer stability to these light bullets. The LLBs of the maximum intensity and losses is consequently the most stable among all LLBs, which acts as an attractor in the self-focusing dynamics with nonlinear losses.

From numerical simulations, we first show that the most lossy light bullet tends to be spontaneously formed in the collapse of standard, Gaussian-like wave packets arrested by NLLs. Of course, the complete formation of this LLB attractor would require infinite amounts of energy. It is then only formed up to a certain maximum radius, depending on the available energy in the initial Gaussian wave packet, and its incomplete formation causes its eventually decay, which takes place through an adiabatic sequence of less dissipative LLBs. For conciseness, we review these results in the case of three-dimensional, or spatiotemporal collapse of ultrashort pulses in media with anomalous dispersion [1]. Similar results for the two-dimensional, spatial collapse of monochromatic light were described in [15].

The dynamics of the spontaneous formation and decay of the most lossy light bullet described by the simple Kerr+NLL model is found to describe the observed facts in the dynamics of light filaments excited by ultrashort pulses in media with anomalous dispersion [13, 14], including the filament intensity, the formation of long fila-

ment segments and repeated collapse in the form of short bursts, which supports the relevance the most lossy light bullet in these filamentation experiments. In this connection, the most lossy three-dimensional light bullet appears here as the counterpart in media with anomalous dispersion of the conical light bullets that are spontaneously formed in media with normal dispersion [18–20], and would constitute an alternate form the so-called light bullets [21–24], or stable, stationary and localized wave packets in all dimensions.

Second, we perform a linearized analysis of instability of LLBs that shows that they are unstable under radial perturbations. The exponential gain of the unstable modes, however, decrease drastically with increasing NLLs, which confirms the stabilizing role of NLLs. In particular, the gain of the most lossy light bullet is found to be negligible or zero, which is in agreement with its attractive property.

### A. The most lossy light bullet as an attractor of the self-focusing dynamics with nonlinear losses

Figure 5 shows the axial evolution of the peak intensity and width when the three-dimensional (spatiotemporal symmetric) Gaussian pulses

$$A = \sqrt{\frac{2P}{\pi s^2}} \exp\left(-\frac{r^2}{s^2}\right), \quad (9)$$

of carrier wavelength  $\lambda_0 = 2\pi c/\omega_0 = 1550$  nm, and of different peak powers  $P$  above the critical peak power for spatiotemporal self-focusing [25],

$$P_{\text{cr}} = \frac{2.157\lambda_0^2}{4\pi n_0 n_2}, \quad (10)$$

are launched in fused silica. The peak intensity and width are evaluated from the numerical solution of the NLSE (1) including only the Kerr and loss nonlinearities. Increasing the energy of the input pulse, the light “segments” of nearly constant high intensity and narrow width become longer, and a number of light “bursts” beyond the segment are formed. These segments may extend beyond the Rayleigh distance  $z_R = \pi s^2/\lambda_0$  of the input pulse, and survive by several hundred times the Rayleigh distance expected from their width. These facts have been observed in self-channelling experiments and numerical simulations [13, 14]. The location and intensity of the segments and bursts in Fig. 5 are even in quantitative agreement with accurate simulations under the same conditions (Fig. 2 in [14]) that include in the NLSE not only Kerr nonlinearity and NLLs, but also all relevant higher-order effects in propagation (space-time focusing, self-steepening, higher-order dispersion and plasma defocusing), and using input Gaussian pulses that are not completely symmetric.

Remarkably, the peak intensity of the segments and bursts reaches a value that is close to the intensity of

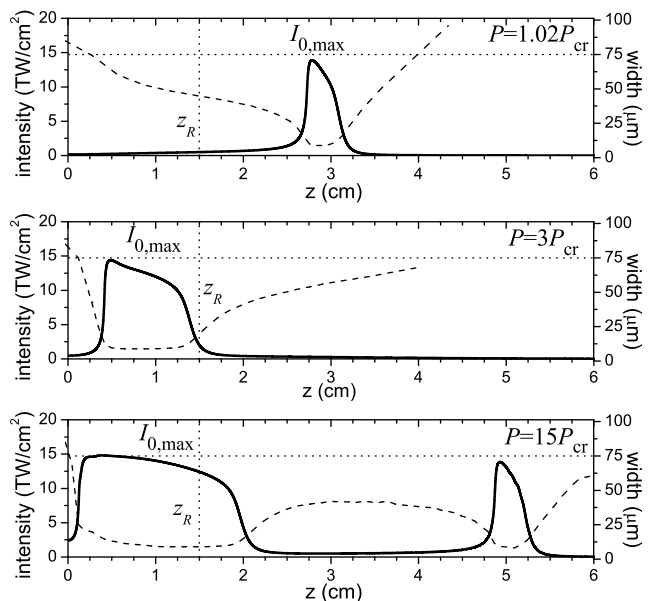


FIG. 5. Peak intensity (solid curves) and FWHM width (dashed blue curves) along  $z$  for input Gaussian pulses of carrier frequency  $\omega_0 = 1.21525$  fs $^{-1}$ , Gaussian width  $s = 0.00716$  cm [duration  $s(k_0|k_0''|)^{1/2} = 29$  fs], and increasing power above the critical power  $P_{\text{cr}} = 13$  MW, calculated from Eq. (1) with the parameters of fused silica ( $k_0 = 5.854 \times 10^4$  cm $^{-1}$ ,  $k_0'' = -279.4$  cm $^{-1}$ fs $^2$ ,  $n_2 = 2.2 \times 10^{-16}$  cm $^2$ /W,  $\beta^{(M)} = 5.11 \times 10^{-116}$  cm $^{17}$ /W $^9$ , with  $M = 10$  [14]).

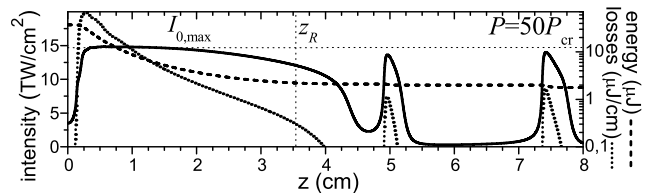


FIG. 6. Peak intensity (solid curve), energy (dashed curve) and losses (dotted curve) along  $z$  in the same conditions as in Fig. 5 except the Gaussian width  $s = 0.011$  cm [Gaussian duration  $s(k_0|k_0''|)^{1/2} = 44.5$  fs] and the peak power  $P = 50P_{\text{cr}}$ .

the LLB with the maximum intensity  $I_{0,\text{max}}$  and infinite losses. The intensity of the segments and burst does not depend on the initial power, as in Figs. 5 from (a) to (c), and of its width, as seen in Fig. 6). Also, in experiments and “exact” numerical simulations of self-focusing in fused silica at the same carrier wave length, the intensity of the long-lived quasi light bullets, or filament segments, is close to the intensity  $I_{0,\text{max}}$  of the most lossy light bullet. Along the segments, however, the pulse energy is drastically decreasing [Fig. 6, dashed curve] due to an energy loss per unit length [Fig. 6, dotted curve] comparable to the total energy. These observations suggest that collapse arrested by NLLs results in the (par-

tial) formation of the LLB of the intensity  $I_{0,\max}$ . Among all possible LLBs with different intensities, the equilibrium between self-focusing and NLLs appears to be more stably reached in the LLB with maximum losses.

Also, the radial intensity profile of the input Gaussian wave packet transforms during the self-focusing stage into the radial profile of most LLB [Fig. 7 (a), solid curves and dashed curves]. Once the intensity is stabilized at about  $I_{0,m}$ , the inner part of the radial profile fits accurately that of the most LLB [Fig. 7(b), solid and dashed curves]. However, the finite energy of the pulse prevents the pulse from reaching completely this bullet attractor. As  $z$  increases, the slowly evolving radial profile along the segment fits successively the profiles of LLBs with slowly changing intensities extremely close to  $I_{0,m}$  [Fig. 7(b), open circles]. At longer propagation distances, the increasingly lack of energy forces the pulse to decay into less dissipative light bullets, endowed momentarily of a very small cone angle. The radial profiles [Fig. 7(c), solid curves] at different values of  $z$  are seen to match now the those of conical light bullets with the same peak intensity and total losses as the propagating pulse [Fig. 7(c), open circles]. Contrary to what is stated in Ref. [15] in the two-dimensional case, the cone angles in the relaxation stage are small but not completely negligible.

Figure 8 offers an overall view of the collapse, filamentation, and relaxation dynamics in the space of parameters of conical light bullets ( $I_0, \theta$ ), and in the subspace of LLBs ( $I_0, \theta = 0$ ). The dashed area indicates the region of parameters where these bullets do not exist. Self-focusing carries the pulse directly to the point  $(I_{0,\max}, 0)$  representing the LLB of maximum losses in fused silica at 1550 wave length, or to points so close to it that they cannot be discerned at the scale of the figure or of the inset, remaining in this vicinity for about the first half of the collapse segment. Relaxation follows the indicated trajectory, where it is seen that the cone angle grows initially, but returns to zero at the end of the segment. The same dynamics explains also the ‘‘bursts’’ after the segments, if any, but since the remaining energy is considerably smaller, the lossy light bullet attractor is less approached and relaxation is faster.

## B. Stability under small perturbations

The attracting property of the most LLB suggests that it must be endowed of certain stability properties. An analysis of stability of these LLBs, as done for other solitons or nonlinear conical waves, turns out to be an insurmountable task because, first, they are known only numerically, and second, and mainly, because they are very weakly localized. We follow instead a simplified procedure, close to that in [26], to show that LLBs become more stable as their intensity and losses increase, the most lossy light bullet being therefore the most stable LLB. The idea that NLLs confer stability has already been expressed in [7] and [27] in relation to conical beams

in media with NLLs. In absence of a conical structure, the spontaneous transformation of Gaussian-like wave packets into the most LLB upon self-focusing reflects the fact that this LLB is the most stable, non-conical, stationary state in a self-focusing medium with NLLs.

To simplify the analysis we use the dimensionless variables  $\tilde{A} = A/\sqrt{I_0}$ ,  $\rho = \sqrt{k_0^2 n_2 I_0/n_0} r$ , and  $\xi = (k_0 n_2 I_0/n_0) z$ , to rewrite the NLSE (1) as

$$\partial_\xi \tilde{A} = \frac{i}{2} \Delta_\rho \tilde{A} + i|\tilde{A}|^2 \tilde{A} - 2\gamma |\tilde{A}|^{2M-2} \tilde{A}, \quad (11)$$

where  $\Delta_\rho = \partial_\rho^2 + [(D-1)/\rho]\partial_\rho$ , and

$$\gamma = \frac{n_0 \beta^{(M)} I_0^{M-2}}{4k_0 n_2}. \quad (12)$$

The equations for LLBs  $\tilde{A} = \tilde{a} \exp[i\varphi]$  become

$$\tilde{a}'' + \frac{D-1}{\rho} \tilde{a}' - (\varphi')^2 \tilde{a} + 2\tilde{a}^3 = 0, \quad (13)$$

$$4\gamma \int_0^\rho d\rho \pi (2\rho)^{D-1} \tilde{a}^{2M} = -\pi (2\rho)^{D-1} \varphi' \tilde{a}^2, \quad (14)$$

where the last equation admits also the differential form

$$\left( \varphi'' + \frac{D-1}{\rho} \varphi' \right) \tilde{a}^2 + \varphi' (\tilde{a}^2)' + 4\gamma \tilde{a}^{2M} = 0, \quad (15)$$

with boundary conditions  $\tilde{a}'(0) = 0$ ,  $\varphi'(0) = 0$  and  $\tilde{a}(0) = 1$ , and the localization condition  $\tilde{a} \rightarrow 0$  for  $\rho \rightarrow \infty$ . The parameter  $\gamma$  ranges from 0 for the lossless case to the value of  $\gamma_{\max}$  of the limiting LLB for the given values of  $D$  and  $M$ .

In a standard, linearized analysis of stability, a weakly perturbed steady state of the form

$$\tilde{A}(\rho, \xi) = \tilde{a}(\rho) e^{i\varphi(\rho)} + \epsilon \left[ u(\rho) e^{i\kappa \xi} + v^*(\rho) e^{-i\kappa^* \xi} \right] \quad (16)$$

is introduced into Eq. (11), and nonlinear terms in the small parameter  $\epsilon$  are disregarded. This leads to the differential eigenvalue problem

$$\begin{pmatrix} H & f \\ -f^* & -H^* \end{pmatrix} \begin{pmatrix} u \\ v \end{pmatrix} = \kappa \begin{pmatrix} u \\ v \end{pmatrix}, \quad (17)$$

where  $H = \frac{1}{2} \Delta + (2\tilde{a}^2 + 2i\gamma M \tilde{a}^{2M-2})$  and  $f = [\tilde{a}^2 + 2i\gamma(M-1)\tilde{a}^{2M-2}]e^{2i\varphi}$ . Stability is determined by the absence of eigenvalues  $\kappa = \kappa_R + i\kappa_I$  with negative imaginary part  $\kappa_I$ , which would lead to an exponential growth with gain  $-\kappa_I$  of the associated eigenmode  $(u, v)$ . Similar eigenvalue problems have been solved numerically in the case of solitons in lossless media. For nonlinear Bessel beams, a numerical solution becomes barely practicable. Due to their persistent tails, a huge radial grid with thousand of points is needed, and truncation, even if weak, tends to falsify the spectrum of eigenvalues. Partial results for the two-dimensional case were nevertheless obtained in Refs. [7, 27] in relation to the stabilizing role

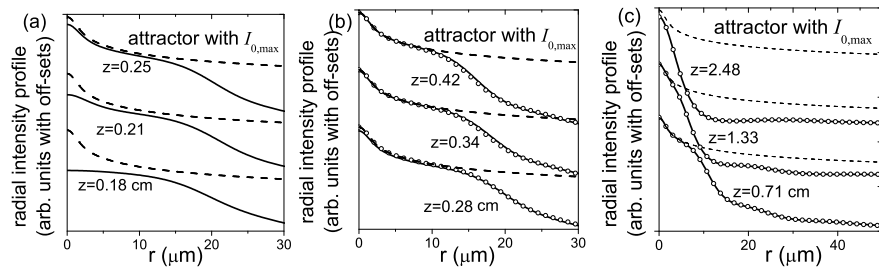


FIG. 7. For the same simulation as in Fig. 6, radial intensity profiles of the pulse at increasing propagation distances  $z$  (solid curves), of the most lossy light bullet (dashed curve) and of the lossy or conical light bullet fitting the pulse (open circles). A vertical off-set is introduced for clarity.

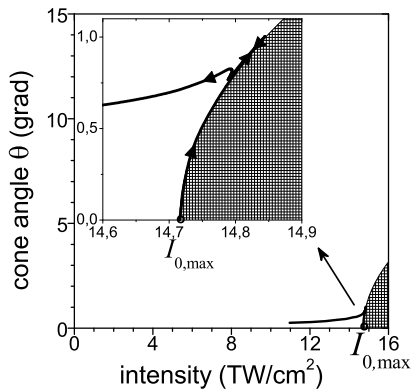


FIG. 8. For the same example as in Figs. 6 and 7, visualization of the evolution as a trajectory in the parameter space of conical and lossy light bullets in fused silica at 1550 nm. The inset shows a tiny region close to  $I_{0,\max}$ .

of losses in these nonlinear Bessel beams. LLBs are even less localized than nonlinear Bessel beams, and these difficulties become overwhelming.

Instead of solving (17), we have followed the simplified procedure of launching weakly perturbed LLBs as initial conditions and letting the possible exponential instability to be manifested. If the initial perturbation is weak enough, all excited unstable modes will grow from very low values, the unstable mode with the highest exponential rate  $-\kappa_I$  will emerge from others at a distance where it is still a small (linear) perturbation, and its eigenvalue  $\kappa$  and shape  $(u, v)$  can be easily extracted.

Truncation of the LLB at a large radius is used as the weak perturbation that onsets instability. Numerical solution of Eq. (11) with these initially truncated LLBs shows exponentially growing harmonic oscillations on their top. For the three-dimensional case and with  $M = 10$ , e.g., Fig. 9(a) shows the axial intensity  $|\tilde{A}(0, \xi)|^2$  for perturbed LLBs with  $\gamma = 0$  (lossless limit) and with  $\gamma = 0.1$ , and Fig. 9(b) shows, in logarithmic scale, the difference  $|\tilde{A}(0, \xi)|^2 - 1$  with respect to the unperturbed propagation. For each specific LLB, the expo-

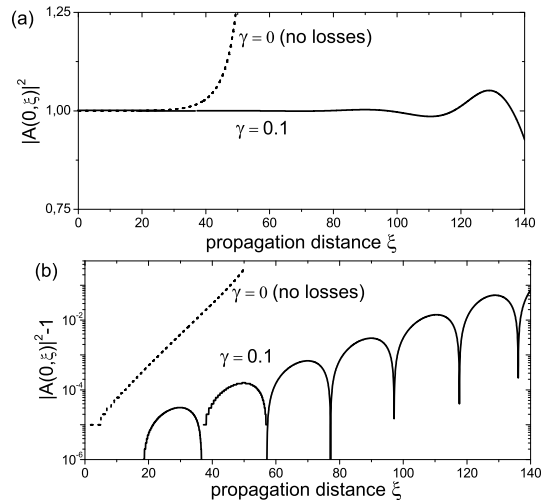


FIG. 9. (a) Normalized axial intensity  $|A(0, \xi)|^2$  and (b) difference  $|A(0, \xi)|^2 - 1$  of initially perturbed (truncated at the large radius  $\rho_t = 1132$ ) three-dimensional LLBs in media with  $M = 0$  and intensities such that  $\gamma \simeq 0$  (dashed curves) and  $\gamma = 0.1$  (solid curves).

nential gain  $-\kappa_I$  and oscillation frequency  $\kappa_R$  is seen to be independent of the initial weak perturbation (different truncation radii). The weaker the input perturbation (the larger the truncation radius), the cleaner the exponentially growing oscillations. As seen in Fig. 9(a), more LLBs preserve its shape for longer propagation distances than less LLBs. This is because the instability gain, i.e., the slope in the logarithmic scale in Fig. 9(b), diminishes with increasing losses. For each LLB (value of  $\gamma$ ), fitting  $|\tilde{A}(0, \xi)|^2 - 1$  with the same quantity given by Eq. (16) in the axial region of small perturbation, allows to obtain the gain  $\kappa_I$  of the dominant unstable mode and its axial oscillation frequency  $\kappa_R$ . They are represented in Figs. 10(a) and (b) as functions of  $\gamma$  for the three-dimensional LLBs with  $M = 10$ . Numerically, it is very difficult to prolong the curves  $\kappa_I - \gamma$  and  $\kappa_R - \gamma$  up to the limit  $\gamma_{\max}$  of the most LLB because LLBs become less and less localized, and the truncation radii must then be extremely



large for the initial perturbation to remain weak. Nevertheless, Fig. 10 evidences the stabilizing role of NLLs. The gain decreases monotonically from its highest value in the limit of negligible losses ( $\gamma = 0$ ) down to negligible or zero when the limit of the most LLB is approached. This result confirms that the most LLB is the most stable light bullet without a conical structure, and explains that it acts as the attractor in the self-focusing and collapse arrested by NLLs of input pulses without a conical structure.

Once the eigenvalue of the dominant unstable mode of each LLB is found, it is not difficult to evaluate its radial shape. Setting Eq. (16) with the propagated fields  $\tilde{A}(\rho, \xi_1)$  and  $\tilde{A}(\rho, \xi_2)$  at two distances in the region of small perturbation, obtained from the NLSE (11), the radial shape of the unstable mode can be evaluated from

$$[u(\rho), v(\rho)] = \frac{g_1 e^{\kappa_I \xi_1} - g_2 e^{\kappa_I \xi_2} e^{\mp \kappa_R (\xi_1 - \xi_2)}}{e^{\pm \kappa_R \xi_1} [1 - e^{2i\kappa_R (\xi_1 - \xi_2)}]}, \quad (18)$$

where the upper (lower) plus-minus signs stand for  $u$  ( $v$ ), and  $g_i = \tilde{A}(\rho, \xi_i) - \tilde{a}(\rho)$ ,  $i = 1, 2$ . Except for small fluctuations, the unstable mode obtained from Eq. (18) is independent of the input weak perturbation and of the couple of distances chosen, which supports the consistency of our instability analysis. As an example, Fig. 11 shows the most unstable mode growing on the top of the three-dimensional LLB with  $M = 10$  and  $\gamma = 0.1$ .

## VII. CONCLUSIONS

Summarizing, we have reviewed the properties of purely nonlinear localized waves sustained by a dynamic equilibrium between self-focusing and nonlinear losses. Their finite-energy versions preserve light bullet behavior well-beyond the diffraction or dispersion distances, and they rebuild after obstacles. Lossy light bullets are essentially multidimensional waves because the replenishment mechanism from the energy reservoir is based solely on

the trend toward collapse, which does not exist with one

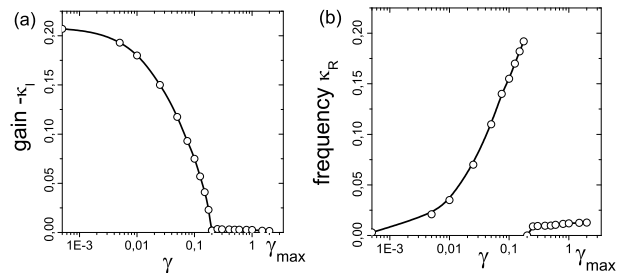


FIG. 10. Normalized exponential gain  $-\kappa_I$  and axial oscillation frequency  $\kappa_R$  of the dominant unstable mode of three-dimensional LLBs with  $M = 10$  as functions of increasing losses  $\gamma$ . In physical units the gain and frequency are  $-(k_0 n_2 I_0 / N_0) \kappa_I$  and  $(k_0 n_2 I_0 / N_0) \kappa_R$ , respectively.

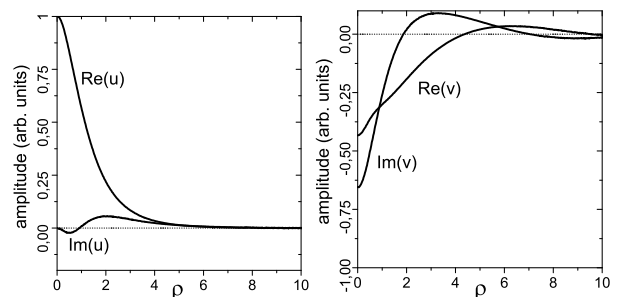


FIG. 11. Parts (a)  $u$  and (b)  $v$  of the dominant unstable eigenmode of the three-dimensional LLB in media with  $M = 10$  and  $\gamma = 0.1$ . Normalization is such that  $\text{Im}(u) = 0$ .

dimension. There is a preferential lossy light bullet with maximum intensity and losses, and defined solely by the optical properties of the medium. This is the most stable, non-conical localized wave sustained by a medium with self-focusing nonlinearity and nonlinear losses, and as such acts as an attractor in the self-focusing dynamics with nonlinear losses of non-conical wave packets, as an input Gaussian wave packet.

- 
- [1] M. A. Porras, “A dissipative attractor in the spatiotemporal collapse of ultrashort light beams,” *Opt. Express* **18**, 7376-7383 (2010).
- [2] M. A. Porras, “Nonlinear light bullets in purely lossy, self-focusing media,” *Appl. Phys. B* **103**, 591-596 (2011).
- [3] J. Durnin, J. J. Miceli, “Diffraction-free beams,” *Phys. Rev. Lett.* **58**, 1499-1501 (1987).
- [4] Z. Bouchal, J. Wagner, and M. Chlup, “Self-reconstruction of a distorted nondiffracting beam,” *Opt. Commun.* **151**, 207-211 (1998).
- [5] A. Dubietis, E. Gaizauskas, G. Tamosauskas, and Paolo Di Trapani, “Light Filaments without Self-Channelling,” *Phys. Rev. Lett.* **92**, 253903 (2004).
- [6] A. Dubietis, E. Kucinskas, G. Tomosaukas, E. Gaizauskas, M.A. Porras, P. Di Trapani, “Self-reconstruction of light filaments,” *Opt. Lett.* **29**, 2893-2895 (2004).
- [7] M. A. Porras, A. Parola, D. Faccio, A. Dubietis, and P. Di Trapani, “Nonlinear unbalanced Bessel beams: Stationary conical waves supported by nonlinear losses,” *Phys. Rev. Lett.* **93**, 153902 (2004).
- [8] M. A. Porras, A. Parola, and P. Di Trapani, “Nonlinear unbalanced O waves: nonsolitary, conical light bullets in nonlinear dissipative media,” *J. Opt. Soc. Am. B* **22**, 1406-1413 (2005).

- [9] N. Akhmediev and A. Ankiewicz (Eds.), *Dissipative solitons*, Lecture Notes in Physics **661**, (Springer, 2005).
- [10] P. Grelu, J. M. Soto-Crespo, and N. Akhmediev, “Light bullets and dynamic pattern formation in nonlinear dissipative systems,” *Opt. Express* **13**, 9352-9360 (2005).
- [11] A. Ankiewicz, N. Devine, N. Akhmediev, and J. M. Soto-Crespo, *Phys. Rev. A* **77**, “Continuously self-focusing and continuously self-defocusing two-dimensional beams in dissipative media,” 033840 (2008).
- [12] S. Henz and J. Herrmann, “Two-dimensional spatial optical solitons in bulk Kerr media stabilized by self-induced multiphoton ionization: Variational approach,” *Phys. Rev. E* **53**, 4092-4097 (1996).
- [13] D. Moll and Alexander L. Gaeta, “Role of dispersion in multiple-collapse dynamics,” *Opt. Lett.* **29**, 995-997 (2004).
- [14] L. Bergé and S. Skupin, “Self-channeling of ultrashort laser pulses in materials with anomalous dispersion,” *Phys. Rev. E* **71**, 065601 (2005).
- [15] M. A. Porras and A. Parola, “Nonlinear unbalanced Bessel beams in the collapse of Gaussian beams arrested by nonlinear losses,” *Opt. Lett.* **33**, 1738-1740 (2008).
- [16] P. Johhanisson, D. Anderson, M. Lisak, M. Marklund, “Nonlinear Bessel beams,” *Opt. Commun.* **222**, 107 (2003).
- [17] D. Faccio, M. Clerici, A. Averchi, O. Jedrkiewicz, S. Tzortzakis, D. Papazoglou, F. Bragheri, L. Tartara, A. Trita, S. Henin, I. Cristiani, A. Couairon, and P. Di Trapani, “Kerr-induced spontaneous Bessel beam formation in the regime of strong two-photon absorption,” *Opt. Express* **16**, 8213-8218 (2008).
- [18] P. Di Trapani, G. Valiulis, A. Piskarskas, O. Jedrkiewicz, J. Trull, C. Conti, and S. Trillo, “Spontaneously generated X-shaped light bullets,” *Phys. Rev. Lett.* **91**, 093904 (2003).
- [19] D. Faccio, M. A. Porras, A. Dubietis, F. Bragheri, A. Couairon, and P. Di Trapani, “Conical emission, pulse splitting, and X-wave parametric amplification in nonlinear dynamics of ultrasort light pulses,” *Phys. Rev. Lett.* **96**, 193901 (2006).
- [20] M. Kolesik, E.M. Wright, and J.V. Moloney, “Dynamic nonlinear X waves for femtosecond pulse propagation in water,” *Phys. Rev. Lett.* **92**, 253901 (2004).
- [21] Y. Silberberg, “Collapse of optical pulses,” *Opt. Lett.* **15**, 1282-1284 (1990).
- [22] F. Wise and P. Di Trapani, “The hunt for light bullets—Spatiotemporal solitons,” *Opt. and Photonics News* 29-32 (2002).
- [23] H. S. Eisenberg, R. Morandotti, and Y. Silberberg, “Kerr spatiotemporal self-Focusing in a planar glass waveguide,” *Phys. Rev. Lett.* **82**, 043902 (2001).
- [24] G. Fibich and B. Ilan, “Optical light bullets in a pure Kerr medium,” *Opt. Lett.* **29**, 887-889 (2004).
- [25] This peak power is slightly higher than the power  $P_{cr} = 2\lambda_0^2/[4\pi n(\omega_0)n_2]$  for spatial self-focusing.
- [26] J. M. Soto-Crespo, D. R. Heatley, E. M. Wright, and N. N. Akhmediev, “Stability of the higher-bound states in a saturable self-focusing medium,” *Phys. Rev. A* **44**, 636-644 (1991).
- [27] P. Polesana, A. Couairon, D. Faccio, A. Parola, M. A. Porras, A. Dubietis, A. Piskarskas, and P. Di Trapani, “Observation of Conical Waves in Focusing, Dispersive, and Dissipative Kerr Media,” *Phys. Rev. Lett* **99**, 223902 (2007).